

Accurate absolute and relative core-level binding energies from GW

Dorothea Golze,* Levi Keller, and Patrick Rinke

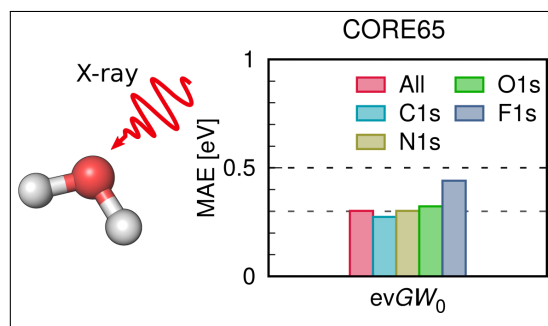
Department of Applied Physics, Aalto University, Otakaari 1, FI-02150 Espoo, Finland

E-mail: dorothea.golze@aalto.fi

Abstract

We present an accurate approach to compute X-ray photoelectron spectra based on the GW Green's function method, that overcomes shortcomings of common density functional theory approaches. GW has become a popular tool to compute valence excitations for a wide range of materials. However, core-level spectroscopy is thus far almost uncharted in GW . We show that single-shot perturbation calculations in the G_0W_0 approximation, which are routinely used for valence states, cannot be applied for core levels and suffer from an extreme, erroneous transfer of spectral weight to the satellite spectrum. The correct behavior can be restored by partial self-consistent GW schemes or by using hybrid functionals with almost 50% of exact exchange as starting point for G_0W_0 . We include also relativistic corrections and present a benchmark study for 65 molecular 1s excitations. Our absolute and relative GW core-level binding energies agree within 0.3 and 0.2 eV with experiment, respectively.

Graphical TOC Entry



Core-level spectroscopy techniques, such as X-ray photoelectron spectroscopy (XPS), are important tools for chemical analysis and can be applied to a broad range of systems including crystalline¹ and amorphous materials,²⁻⁴ liquids,⁵⁻⁷ adsorbates at surfaces⁸ or 2D materials.^{9,10} XPS measures core-level binding energies (BEs), which are element-specific, but depend on the local chemical environment. For complex materials, the assignment of the experimental XPS signals to the specific atomic sites is notoriously difficult, due to overlapping spectral features or the lack of well-defined

reference data.³ Accurate theoretical tools for the prediction of core excitations are therefore important to guide the experiment. Calculated *relative* binding energies, i.e., BE shifts with respect to a reference XPS signal, are particularly useful for the interpretation of experimental spectra. However, the prediction of accurate *absolute* core-level energies is equally important, in particular when reference core-level energies are not available.

The most common approach to compute core-level BEs is the Delta self-consistent field (Δ SCF) method, which is

based on Kohn-Sham density functional theory (KS-DFT). In Δ SCF, the core-level binding energies are calculated as total energy difference between the neutral and the ionized system.¹¹ Relative core-level BEs from Δ SCF generally compare well to experiment. For small molecules, deviations typically lie in the range of 0.2 – 0.3 eV,¹² which is well within or close to the chemical resolution required for most elements. The dependence of the relative BEs on the exchange-correlation (XC) functional is almost negligible for small systems,¹² but can be more severe for complex materials.^{10,13} Absolute Δ SCF BEs can differ by several eV from the experimental data. This deviation is quite sensitive to the XC-functional.¹⁴ The best results for absolute core excitations have been obtained using the TPSS¹⁵ and SCAN¹⁶ meta-generalized gradient approximations. The reported mean absolute deviations from experiment lie in the range of ≈ 0.2 eV for benchmark sets of small molecules. For medium-sized to large molecules, however, the accuracy of Δ SCF can quickly reduce by an order of magnitude for absolute BEs.¹⁷ This behavior can be partly attributed to an insufficient localization of the core hole in the calculation for the ionized system. Constraining the core hole in a particular state can be difficult and variational instabilities are not uncommon.¹⁸

Most importantly, Δ SCF cannot be applied without further approximations to periodic systems, such as surfaces, where the ionized calculation would lead to a Coulomb divergence.¹⁹ Such divergences can be circumvented by using cluster models,²⁰ by neutralizing the unit or supercell with compensating background charges²¹ or by adding the compensating electrons to the conduction band.^{22–24} However, these approximations can obscure the calculations and even lead to qualitatively wrong results, as recently demonstrated for oxide surfaces.²⁵

Higher-level theoretical methods such as Delta coupled-cluster (Δ CC) approaches yield highly accurate relative and absolute core ionization energies.^{26–28} Δ CC also requires the computation of a core-ionized system leading to the same conceptual problems as in Δ SCF. Response theories, e.g., equation-of-motion coupled cluster, avoid these problems, but deviate by several eV from experiment and require at least triples contributions for quantitative agreement.²⁹ Good accuracy for deep states was reported for a recently introduced direct approach based on effective one-particle energies from the generalized KS random phase approximation.³⁰ However, the application of these higher-level methods is restricted to small or medium-sized systems due to unfavorable scaling with system size and large computational prefactors.

The GW approximation to many-body perturbation theory³¹ is a promising method to improve upon the limitations of traditional Δ -approaches and has become a widespread

tool for the accurate prediction of electron removal energies of valence states in molecular and solid-state systems.³² GW is routinely applied to systems with several hundred atoms,^{33–35} and recently even to system sizes with more than 1000 atoms.^{36,37} However, core-level spectroscopy has been rarely attempted with GW . Recently, the first promising results were obtained for solid-state systems.^{38,39} The few existing studies for molecular core excitations give a mixed first impressions since anything between 0.5 eV¹⁷ and 10 eV deviation from experiment has been reported.^{30,40} In this work, we show how reliable and highly accurate core-level BEs can be obtained from GW and explain why large deviations from experiment were reported earlier. We also present a GW benchmark set for 1s core states complementary to the popular $GW100$ benchmark set⁴¹ for valence excitations.

First, we introduce the GW framework. The central object of GW is the self-energy Σ , which contains all quantum mechanical exchange and correlation interactions of the hole created by the excitation process and its surrounding electrons. The self-energy is calculated from the Green’s function G and the perturbation expansion in the screened Coulomb interaction W as formulated by Hedin in the 1960s.³¹ The poles of G directly correspond to the excitation energies as measured in photoemission spectroscopy.

In practice, GW is performed within the first-order perturbation theory (G_0W_0) and starts from a set of mean-field single-particle orbitals $\{\psi_n\}$ and corresponding eigenvalues $\{\varepsilon_n\}$. These are usually obtained from a preceding KS-DFT or Hartree-Fock (HF) calculation. The GW quasiparticle (QP) energies $\varepsilon_n^{G_0W_0}$ are computed by iteratively solving

$$\varepsilon_n^{G_0W_0} = \varepsilon_n + \text{Re} \langle \psi_n | \Sigma(\varepsilon_n^{G_0W_0}) - v^{\text{xc}} | \psi_n \rangle, \quad (1)$$

for $\varepsilon_n^{G_0W_0}$, where v^{xc} is the XC potential from DFT and spin variables are omitted. In the following, we use the notation $\Sigma_n = \langle \psi_n | \Sigma | \psi_n \rangle$ and $v_n^{\text{xc}} = \langle \psi_n | v^{\text{xc}} | \psi_n \rangle$ for the (n, n) diagonal matrix elements of the self-energy and XC potential. The QP energies are related to the BE of state n by $\text{BE}_n = -\varepsilon_n^{G_0W_0}$ and the self-energy Σ is given by

$$\Sigma(\mathbf{r}, \mathbf{r}', \omega) = \frac{i}{2\pi} \int d\omega' e^{i\omega'\eta} G_0(\mathbf{r}, \mathbf{r}', \omega + \omega') W_0(\mathbf{r}, \mathbf{r}', \omega') \quad (2)$$

where η is a positive infinitesimal. The self-energy is typically split into a correlation Σ^c and an exchange part Σ^x , $\Sigma = \Sigma^c + \Sigma^x$, where Σ^c is computed from $W_0^c = W_0 - v$ and Σ^x from the bare Coulomb interaction v . The mean-field Green’s function G_0 is given by

$$G_0(\mathbf{r}, \mathbf{r}', \omega) = \sum_m \frac{\psi_m(\mathbf{r})\psi_m(\mathbf{r}')}{\omega - \varepsilon_m - i\eta \text{sgn}(\varepsilon_F - \varepsilon_m)}, \quad (3)$$

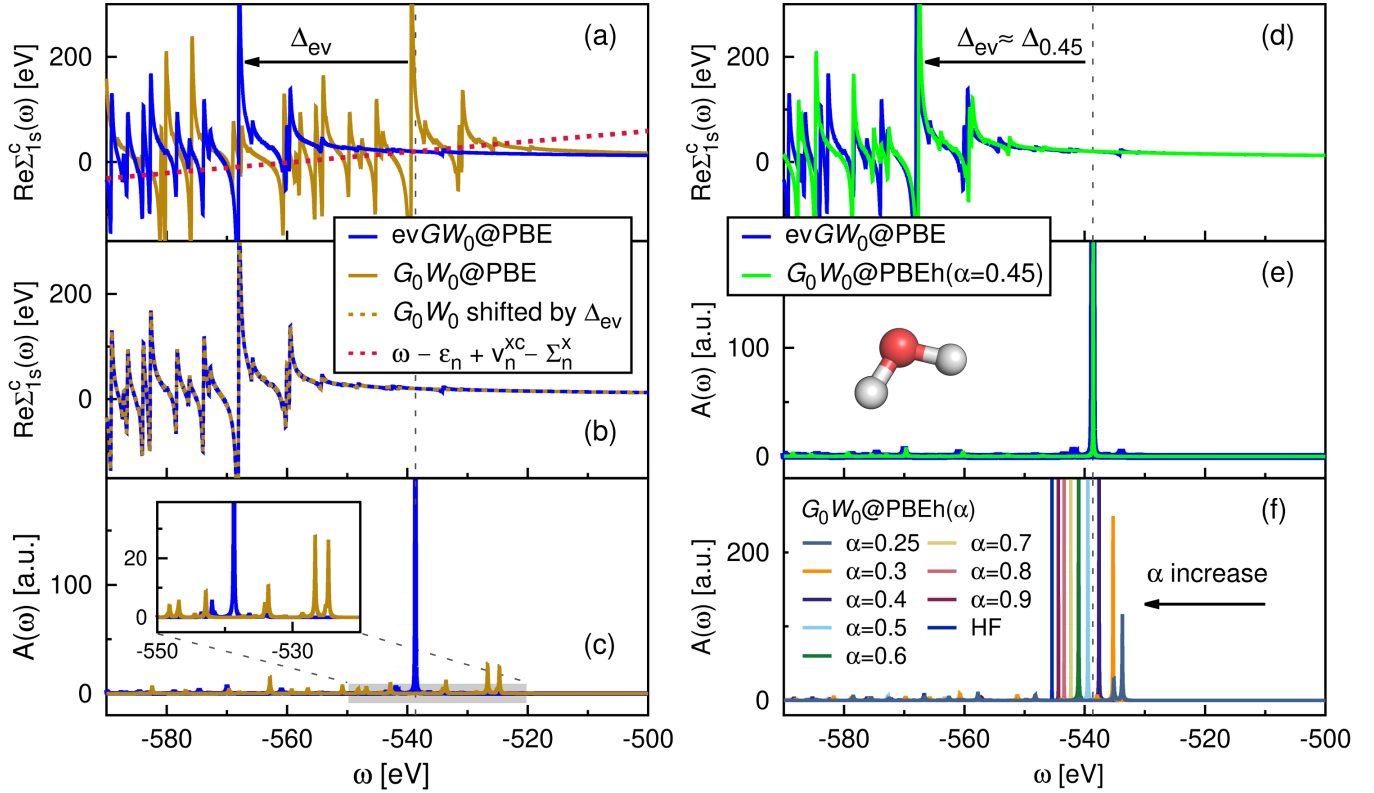


Figure 1: Core excitation for a single water molecule from G_0W_0 and evG_0W_0 . (a) Real part of the self-energy $\Sigma^c(\omega)$ (correlation contribution) using the PBE functional as starting point. Diagonal matrix elements $\text{Re}\Sigma_n^c(\omega) = \langle \psi_n | \text{Re}\Sigma^c(\omega) | \psi_n \rangle$ for the oxygen 1s orbital. (b) Self-energy from $G_0W_0@PBE$ shifted by Δ_{ev} relative to the evG_0W_0 result. The intersection with the red dashed line is the graphical solution of the QP Equation (1). (c) Spectral function $A(\omega)$ from $G_0W_0@PBE$ and $evG_0W_0@PBE$. (d) Self-energy and (e) spectral function using $PBEh(\alpha = 0.45)$ as starting point. (f) Spectral function obtained from $G_0W_0@PBEh$ for different amounts of exact exchange α . The vertical gray-dashed line indicates the QP solution from $evG_0W_0@PBE$. Note that the self-energy is slightly broadened for better visualization and that each sharp peak actually corresponds to a pole.

where ε_F denotes the Fermi energy. W_0 in Equation (2) is the screened Coulomb interaction in the random-phase approximation (RPA) and is computed from the dielectric function as described in Ref. 32.

We now discuss the application of GW to core-level spectroscopy. The basic requirement to obtain computational XPS data from GW is an explicit description of the core electrons. We treat the latter efficiently by working in a local all-electron basis of numeric-atomic centered orbitals (NAOs). Furthermore, we showed that highly accurate frequency integration techniques for the computation of the self-energy (Equation (2)) are required for core states.¹⁷ Unlike for valence states, the self-energy has a complicated structure with many poles in the core region, as displayed in Figure 1(a). For such complex pole structures, the analytic continuation, that is frequently employed in GW calculations for valence states to continue Σ^c from the imaginary to the real frequency axis, fails completely.¹⁷ We showed that the contour deformation (CD) technique, in which a full-frequency integration on

the real frequencies axis is performed, yields the required accuracy. Results from CD exactly match the computationally demanding fully analytic solution of Equation (2).¹⁷ Our CD- GW implementation is computationally efficient enabling the computation of system sizes exceeding 100 atoms, see Ref. 17 for details of our GW core-level implementation in the all-electron code FHI-aims.⁴² Numerically stable and precise algorithms for the computation of the self-energy are only the first step toward reliable core-level excitations from GW . In the following, the failure of standard G_0W_0 schemes for core states is explored.

Figure 1(a) shows the G_0W_0 self-energy matrix elements for the O1s state of an isolated water molecule using the Perdew-Burke-Ernzerhof (PBE)⁴³ functional for the underlying DFT calculation ($G_0W_0@PBE$). Instead of iterating Equation (1), we can obtain its solution graphically by finding the intersections of the straight line $\omega - \varepsilon_n + v_n^{xc} - \Sigma_n^x$ with the self-energy matrix elements Σ_n^c . As apparent from Figure 1(a), a

clear single solution is missing. Many intersections are observed, which are all valid solutions of Equation (1).

To further investigate this multi-solution behavior, we calculate the spectral function $A(\omega)$ ^{17,32}

$$A(\omega) = \frac{1}{\pi} \sum_m \frac{[\text{Im} \Sigma_m(\omega)]}{[\omega - \varepsilon_m - (\text{Re} \Sigma_m(\omega) - v_m^{xc})]^2 + [\text{Im} \Sigma_m(\omega)]^2} \quad (4)$$

where we include also the imaginary part of the complex self-energy and use, unlike in fully self-consistent GW ,^{44,45} only the diagonal matrix elements of Σ . The spectral function for the oxygen 1s excitation of an isolated water molecule is reported in Figure 1(c). We observe many peaks with similar spectral weight. No distinct peak can be assigned to the QP excitation. In other words, $G_0W_0@PBE$ does not provide a unique QP solution for the 1s excitation. This is in sharp contrast to the valence case, where $G_0W_0@PBE$ is routinely applied to molecules and a clear single solution has been reported in the vast majority of cases.⁴¹

Figure 1(c) illustrates that for core states, the QP energy and the satellite spectrum have merged. Satellites are, e.g., due to multi-electron excitations such as shake-up processes^{46,47} and have typically much smaller spectral weights than the QP peak. The fact that we observe the opposite for $G_0W_0@PBE$ implies that almost all spectral weight has been transferred from the QP peak to the satellites. We will next investigate the origin of this behavior and provide a solution.

We start by updating the KS eigenvalues $\{\varepsilon_m\}$ in the Green's function with the G_0W_0 quasiparticle energies, re-evaluate Equation (1) and iterate until G is self-consistent in the eigenvalues. For most valence and virtual states, a unique QP solution exists at the G_0W_0 level, while for core states we initialize the iteration in G with an approximation of the QP energy. This procedure yields a partially eigenvalue self-consistent scheme denoted as $evGW_0@PBE$, where W is kept fixed at the W_0 level. Iterating the eigenvalues in G shifts the onset of the pole structure of the self-energy to lower energies, see Figure 1(a). The pole structure of the self-energy looks similar in $G_0W_0@PBE$ and $evGW_0@PBE$, but shifted by a constant amount. Figure 1(b) shows, that the $G_0W_0@PBE$ self-energy is indeed almost identically to $evGW_0@PBE$ when shifted by $\Delta_{ev} = -28.7$ eV. The effect of this shift is that the graphical solution now produces a clear QP solution and a satellite spectrum with much lower intensity, as displayed in Figure 1(c). In other words, eigenvalue self-consistency in G achieves a separation of QP peak and satellite spectrum for deep core states. This eigenvalue self-consistency strategy was already employed for $3d$ states in transition metal oxides^{48,49} or semi-core states in sodium³⁸ and can be understood as follows.

Satellites occur in frequency regions, where the real part of Σ_n^c has poles and its imaginary part complementary peaks, which is shown in detail in our recent GW review article.³² As obvious from Equation (4), large imaginary parts correlate with low spectral weights, i.e., satellite character. Rewriting the self-energy into analytic form reveals its pole-structure

$$\Sigma_n^c(\omega) = \sum_m \sum_s \frac{\langle \psi_n \psi_m | P_s | \psi_m \psi_n \rangle}{\omega - \varepsilon_m + (\Omega_s - i\eta) \text{sgn}(\varepsilon_F - \varepsilon_m)}, \quad (5)$$

where Ω_s are charge neutral excitations and P_s transition amplitudes.³² The G_0W_0 self-energy therefore has poles at $\varepsilon_i - \Omega_s$ and $\varepsilon_a + \Omega_s$, where i indicates occupied and a virtual states. Each of these poles gives rise to satellite features and can be understood as an electron or hole excitation coupled to a neutral excitation.

For $G_0W_0@PBE$, ε_i are PBE eigenvalues and Ω_s are close to PBE eigenvalue differences between occupied and virtual states. The neutral excitations Ω_s are typically underestimated at the PBE level, while the eigenvalues are overestimated by several eV in the valence region of the spectrum and by 20 to 30 eV for the 1s core states.^{17,40} The $\varepsilon_{1s} - \Omega_s$ poles in the self-energy are therefore considerably too high in energy and start to energetically overlap with the QP energy of the core state. This explains why the satellites have such high spectral weight in $G_0W_0@PBE$ and why no distinct QP peak can be found.

In $evGW_0$, we replace the KS-DFT eigenvalues $\{\varepsilon_m\}$ in Equation (3) by $\varepsilon_m + \Delta\varepsilon_m$, where $\Delta\varepsilon_m$ is the GW correction. For a PBE starting point, $\Delta\varepsilon_m$ is negative for occupied states and the poles of Σ_n^c shift to lower energies, away from the QP energy. The poles in the core region are now located at $\varepsilon_{1s} + \Delta\varepsilon_{1s} - \Omega_s$ and the corresponding satellite peaks are separated from the QP peak and reduced in spectral weight.

The effect of self-consistency in G can be reproduced in a G_0W_0 calculation, which is computationally less demanding, by including exact exchange in the DFT functional. We employ the PBE-based hybrid (PBEh) functional family,⁵⁰ which is characterized by an adjustable fraction α of HF exchange and corresponds for $\alpha = 0.25$ to the PBE0^{51,52} functional. For $\alpha = 0.45$, we obtain approximately the same shift of the pole structure as in $evGW_0@PBE$ and observe a distinct QP peak at the same frequency, see Figure 1(d) and (e). Increasing the amount of exact exchange, the QP peak in the spectral function moves to lower energies, which is in agreement with the starting point optimization studies conducted for valence excitations.^{32,50,53} However, distinct QP peaks are only obtained for $\alpha > 0.3$. As shown Figure 1(f), $G_0W_0@PBE0$ still suffers from a large transfer of spectral weight to the satellites.

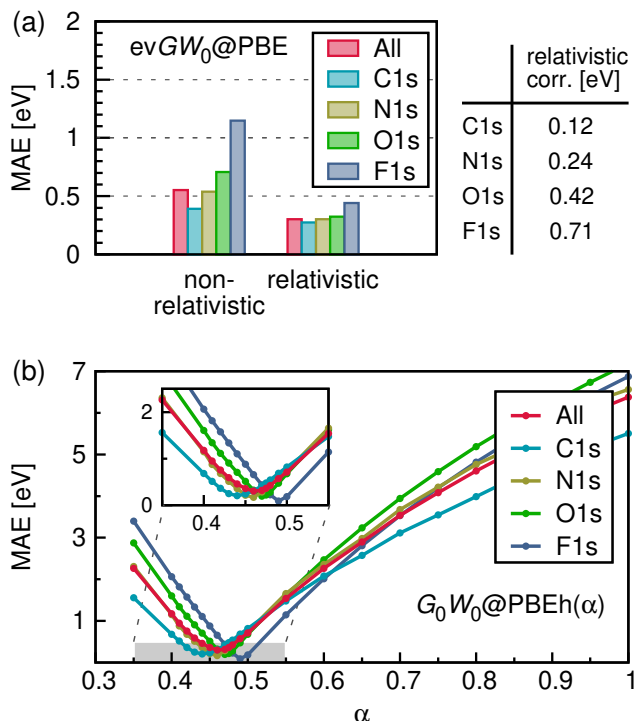


Figure 2: Mean absolute error (MAE) of the absolute BEs for the CORE65 benchmark set with respect to experiment. (a) $evGW_0@PBE$ with and without relativistic correction. (b) MAE for $G_0W_0@PBEh(\alpha)$ dependent on the amount of exact exchange α in the PBEh functional. Relativistic corrections are included.

Previous GW core-level studies for small molecules^{30,40} reported G_0W_0 calculations performed on top of generalized gradient approximation (GGA) or hybrid functionals with a low amount of exact exchange. Our analysis presented in this article demonstrates that those studies cannot have found the QP solution because their spectral function would look like the yellow spectrum in Figure 1(c). Linearizing the QP equation by a Taylor expansion to first-order around ϵ_n , as done in Refs. 30, 40 and 54, for such a spectral function leads to uncontrollable results, which partly explains the large deviation of the reported results from experiment.^{30,40} Furthermore, the linearization error increases rapidly with increasing binding energy and may already amount to 0.5 eV for deeper valence states, as shown in Ref. 32. As already pointed out in our previous work,¹⁷ Equation (1) should always be solved iteratively for core states.

We now assess the accuracy of $evGW_0@PBE$ and $G_0W_0@PBEh$ with respect to experiment for a benchmark set of 65 1s binding energies of gas-phase molecules, denoted in the following as CORE65. This benchmark set contains 30 C1s, 21 O1s, 11 N1s and 3 F1s excitations from 32 small, inorganic and organic molecules up to 14 atoms, see Table S1

in the Supporting Information (SI) for details. The CORE65 benchmark covers a variety of different chemical environments and bonding types and the most common functional groups. As with all correlated electronic structure methods, GW converges slowly with respect to basis set size.³² Even at the quadruple- ζ level, the BEs deviate by 0.2 eV to 0.4 eV from the complete basis set limit (see Tables S2 and S3 in SI). All GW results are thus extrapolated to the complete basis set limit using the Dunning basis set family cc-pVnZ ($n=3-6$).^{55,56}

Since we expect relativistic effects to become important for heavier elements, we add relativistic corrections for the 1s excitations as post-processing step to the GW calculation. Our relativistic corrections have been obtained by solving the radial KS and 4-component Dirac-KS equations self-consistently for a free neutral atom at the PBE level, and evaluating the difference between their 1s eigenvalues; see Figure 2(a). Details of our relativistic correction scheme, which is similar to the one reported in Ref. 15, and its comparison to other relativistic methods will be described in a forthcoming paper.

For $evGW_0@PBE$, the mean absolute error (MAE) of the absolute BEs with respect to experiment is reported in Figure 2(a) for relativistic and non-relativistic calculations. We find that relativistic effects start to dominate the error in the QP energies already for second-row elements. In the non-relativistic case, the core-level BEs are generally underestimated (see Table S2 in the SI) and the MAE increases with the atomic number. Accounting for relativistic effects, the species dependence in the MAE is largely eliminated.

Figure 2(b) shows the MAE at the $G_0W_0@PBEh(\alpha)$ level with respect to the amount of exact exchange α in the PBEh functional, including relativistic corrections. These α dependent calculations are performed for a subset of 43 excitations of the CORE65 benchmark set, for which the mapping between core state and atom is trivial and requires no analysis of, e.g., molecular orbital coefficients. The smallest MAE is obtained for α values around 0.45. This observation agrees nicely with our analysis of the self-energy in Figure 1(d), where we found that $\alpha \approx 0.45$ reproduces the $evGW_0$ self-energy best. For smaller α values, the BEs are underestimated and for larger values increasingly overestimated. The species dependence of the optimal α values are mostly reduced when taking relativistic effects into account. The optimal α values increase only slightly with the atomic number ranging from 0.44 to 0.49, see Figure 2(b).

Figure 3 compares the absolute BEs obtained from experiment to the theoretical BEs computed at the Δ SCF, $evGW_0@PBE$ and $G_0W_0@PBEh(\alpha = 0.45)$ level. The Δ SCF calculations are performed with the PBE0^{51,52} functional and

Table 1: Mean absolute error (MAE) in [eV] with respect to experiment for the CORE65 benchmark set. MAE for absolute and relative core-level BEs, where the latter is the shift of the BE with respect to a reference molecule. CH_4 , NH_3 , H_2O and CH_3F have been used as reference molecules for C1s, N1s, O1s and F1s respectively. Relativistic effects are accounted for in all three methods.

core-level	ΔSCF		$\text{evGW}_0@\text{PBE}$		$G_0W_0@\text{PBEh}(\alpha=0.45)$	
	absolute BEs	relative BEs	absolute BEs	relative BEs	absolute BEs	relative BEs
all	0.33	0.14	0.30	0.18	0.33	0.26
C1s	0.36	0.10	0.27	0.18	0.24	0.29
N1s	0.32	0.08	0.30	0.14	0.16	0.23
O1s	0.32	0.22	0.32	0.22	0.48	0.25
F1s	0.12	0.13	0.44	0.05	0.83	0.11

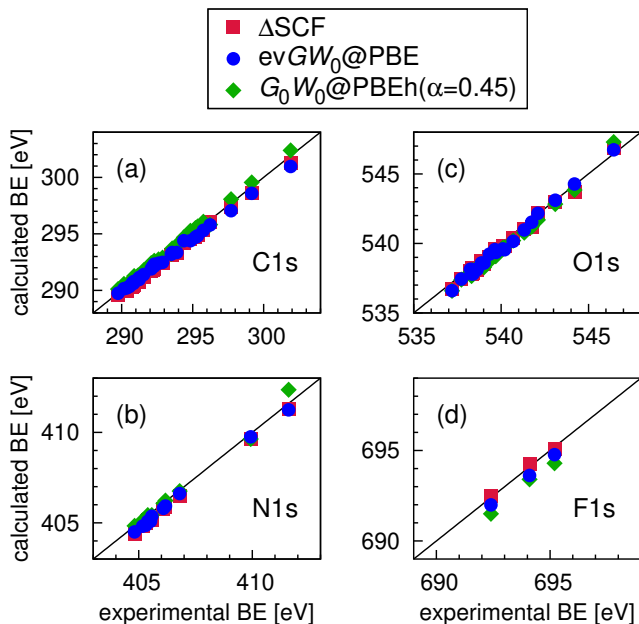


Figure 3: Absolute C1s (a), N1s (b), O1s (c) and F1s (d) binding energies (BEs) for the CORE65 benchmark set comparing calculated values at the ΔSCF , $\text{evGW}_0@\text{PBE}$ and $G_0W_0@\text{PBEh}(\alpha = 0.45)$ level to experiment. The respective computational method underestimates the BE when the data point is below the black line and overestimates when above.

are carefully converged adding additional tight basis functions to standard Gaussian basis sets for the core-hole calculation.⁵⁷ Following a recently proposed ΔSCF simulation protocol,¹⁶ we include scalar relativistic effects self-consistently via the zeroth order regular approximation (ZORA).⁵⁸ Our BEs obtained from ΔSCF -PBE0 agree with an overall MAE of 0.33 eV much better with experiment than reported in previous studies (0.7 eV),¹⁴ which must be attributed to incomplete basis sets and the neglect of relativistic effects.

The $\text{evGW}_0@\text{PBE}$ approach yields excellent agreement of the absolute BEs with experiment consistently for all data points as shown in Figure 3. With an overall MAE of 0.3 eV,

the accuracy of $\text{evGW}_0@\text{PBE}$ is well within the chemical resolution required for the interpretation of most XPS spectra. $G_0W_0@\text{PBEh}(\alpha = 0.45)$ yields a similar overall MAE, which, however, depends to some extent on the species, see Table 1. As shown in Figure 3(d), F1s removal energies are systematically underestimated with $G_0W_0@\text{PBEh}$. Results for this element could in principle be improved by using an element-specific optimized α value, based on the analysis in Figure 2(b).

Relative BEs are very well reproduced with all three theoretical methods, as shown in Table 1 and in more detail in Figure S1 (SI). With ΔSCF and $\text{evGW}_0@\text{PBE}$ we obtain MAEs smaller than 0.2 eV and slightly larger errors between 0.2 and 0.3 eV with $G_0W_0@\text{PBEh}(\alpha = 0.45)$. Results for F1s are reported for the sake of completeness. However, note that we have only two data points for the relative BEs and the experimental uncertainties are generally larger for fluorine than for the lighter elements. Except for F1s BEs, the MAEs are not species dependent.

In summary, we showed that GW is a reliable and accurate method to calculate 1s core excitations. However, standard G_0W_0 setups routinely used for valence excitations cannot be employed. For core states, G_0W_0 calculations starting from GGA or standard hybrid functionals experience a huge weight transfer from the quasiparticle to the satellites. In fact, this weight transfer is so extreme that a unique QP solution does not exist for the molecules we have investigated. We demonstrated for a PBE starting point that eigenvalue self-consistency in G is mandatory to achieve a proper separation between QP and satellite peaks in the GW calculation. The effects of evGW_0 can be reproduced in G_0W_0 , which is computationally less expensive, by using a hybrid functional with a high fraction of exact exchange as starting point. We found that 45% of HF exchange is optimal. Furthermore, the inclusion of relativistic effects and a proper extrapolation to the complete basis limit are crucial to obtain accurate core-level BEs. Our work is an important stepping stone for the accu-

rate calculation of XPS spectra of condensed systems, where Δ -based approaches face conceptual limitations. GW can be applied without restrictions to systems with periodic boundary conditions and is also for large molecular structures a reliable and numerically robust method. Furthermore, this work is fundamental for the calculation of X-ray absorption spectra (XAS) from the Bethe-Salpeter equation,⁵⁹ which uses the GW results as input.

Computational Details

All calculations are performed with the FHI-aims program package,^{42,60,61} where the all-electron KS equations are solved in the NAO scheme. The structures of the CORE65 molecules have been optimized at the DFT level using NAOs of tier 2 quality⁴² to represent core and valence electrons. The PBE functional⁴³ is used to model exchange and correlation in combination with the atomic ZORA^{42,58} kinetic energy operator. Van der Waals interactions are accounted for by employing the Tkatchenko-Scheffler dispersion correction.⁶²

Core-level BEs from Δ SCF are calculated using the PBE0^{51,52} hybrid functional, (atomic) ZORA and def2 quadruple- ζ valence plus polarization (def2-QZVP)⁶³ basis sets. The def2-QZVP basis sets are all-electron basis sets of contracted Gaussian orbitals, which are optimized to yield accurate total energies.⁶³ Gaussian basis sets can be considered as a special case of an NAO and are treated numerically in FHI-aims. To guarantee the full relaxation of other electrons in the presence of the core hole, we decontracted the def2-QZVP basis sets in the Δ SCF calculation to add tighter core functions. To properly localize the core hole at a specific atom, we performed a Boys localization⁶⁴ at the end of the SCF cycle of the charge neutral calculation and used this wavefunction as initial guess for the charged system.

For the GW calculations, we use the contour deformation technique^{17,32,33,65} to evaluate the frequency integral of the self-energy and employ a modified Gauss-Legendre grid⁶¹ with 200 grid points for the imaginary frequency integral. The QP equation is *always* solved iteratively. For $evGW_0$, we iterate additionally the QP energies in G including explicitly all occupied states and the first five virtual states in the iteration. Scissor shifts are employed for the remaining virtual states. For the partially self-consistent $evGW_0$ calculations, we use the PBE functional as starting point and for $G_0W_0@PBEh(\alpha)$ calculations the $PBEh(\alpha)$ hybrid functionals.⁵⁰ The core-level BEs are extrapolated to the complete basis set limit using the Dunning basis set family cc-pVnZ ($n=3-6$),^{55,56} which are standard basis sets for correlated electronic-structure methods. The extrapolation has been performed with four points by a linear regression against the inverse of the total number

of basis functions. The standard error of the extrapolation is smaller than 0.1 eV and the correlation coefficient R^2 in most cases > 0.9 , see Table S2 and S3 in the SI. Alternatively, the extrapolation can be performed with respect to C_n^{-3} , where C_n is the cardinal number of the basis set. We found that the difference between both extrapolation schemes is very small, e.g., the average absolute deviation is only 0.04 eV for the CORE65 $G_0W_0@PBEh(\alpha=0.45)$ data. Self-energy matrix elements and spectral functions are calculated at the cc-pV4Z level. The relativistic corrections for the GW energies are computed at the PBE level from free neutral atom calculations on numerical real space grids.⁶⁶

Acknowledgement We thank the CSC - IT Center for Science for providing computational resources. D. Golze acknowledges financial support by the Academy of Finland (Grant No. 316168). We thank Lucia Reining, Michiel van Setten and Volker Blum for fruitful discussions.

Supporting Information Available

The following files are available free of charge. Plot of relative core-level BEs comparing theory and experiment (Figure S1); CORE65 benchmark results at the Δ SCF, $evGW_0@PBE$ and $G_0W_0@PBEh(\alpha=0.45)$ level including relativistic corrections and experimental data (Table S1 and Figure S2); non-relativistic $evGW_0@PBE$ and $G_0W_0@PBEh(\alpha=0.45)$ results for basis set series cc-pVnZ ($n=3-6$), extrapolated values, standard errors and correlation coefficients (Table S2 and S3); structures of CORE65 benchmark set.

References

- (1) Bagus, P. S.; Ilton, E. S.; Nelin, C. J. The interpretation of XPS spectra: Insights into materials properties. *Surf. Sci. Rep.* **2013**, *68*, 273–304.
- (2) Sainio, S.; Nordlund, D.; Caro, M. A.; Gandhiraman, R.; Koehne, J.; Wester, N.; Koskinen, J.; Meyyappan, M.; Laurila, T. Correlation between sp^3 -to- sp^2 Ratio and Surface Oxygen Functionalities in Tetrahedral Amorphous Carbon (ta-C) Thin Film Electrodes and Implications of Their Electrochemical Properties. *J. Phys. Chem. C* **2016**, *120*, 8298–8304.
- (3) Aarva, A.; Deringer, V. L.; Sainio, S.; Laurila, T.; Caro, M. A. Understanding X-ray spectroscopy of carbonaceous materials by combining experiments,

- density functional theory and machine learning. Part I: fingerprint spectra. *Chem. Mater.* **2019**, in press, DOI:10.1021/acs.chemmater.9b02049.
- (4) Aarva, A.; Deringer, V. L.; Sainio, S.; Laurila, T.; Caro, M. A. Understanding X-ray spectroscopy of carbonaceous materials by combining experiments, density functional theory and machine learning. Part II: quantitative fitting of spectra. *Chem. Mater.* **2019**, in press, DOI:10.1021/acs.chemmater.9b02050.
 - (5) Cremer, T.; Kolbeck, C.; Lovelock, K. R. J.; Paape, N.; Wölfel, R.; Schulz, P. S.; Wasserscheid, P.; Weber, H.; Thar, J.; Kirchner, B.; Maier, F.; Steinrück, H.-P. Towards a Molecular Understanding of Cation-Anion Interactions-Probing the Electronic Structure of Imidazolium Ionic Liquids by NMR Spectroscopy, X-ray Photoelectron Spectroscopy and Theoretical Calculations. *Chem. Eur. J.* **2010**, *16*, 9018–9033.
 - (6) Villar-Garcia, I. J.; Smith, E. F.; Taylor, A. W.; Qiu, F.; Lovelock, K. R. J.; Jones, R. G.; Licence, P. Charging of ionic liquid surfaces under X-ray irradiation: the measurement of absolute binding energies by XPS. *Phys. Chem. Chem. Phys.* **2011**, *13*, 2797–2808.
 - (7) Santos, A. R.; Blundell, R. K.; Licence, P. XPS of guanidinium ionic liquids: a comparison of charge distribution in nitrogenous cations. *Phys. Chem. Chem. Phys.* **2015**, *17*, 11839–11847.
 - (8) Di Giovannantonio, M.; Deniz, O.; Urgel, J. I.; Widmer, R.; Dienel, T.; Stolz, S.; Sánchez-Sánchez, C.; Muntwiler, M.; Dumslaff, T.; Berger, R.; Narita, A.; Feng, X.; Müllen, K.; Ruffieux, P.; Fasel, R. On-Surface Growth Dynamics of Graphene Nanoribbons: The Role of Halogen Functionalization. *ACS Nano* **2018**, *12*, 74–81.
 - (9) Scardamaglia, M.; Susi, T.; Struzzi, C.; Snyders, R.; Di Santo, G.; Petaccia, L.; Bittencourt, C. Spectroscopic observation of oxygen dissociation on nitrogen-doped graphene. *Sci. Rep.* **2017**, *7*, 7960.
 - (10) Susi, T.; Scardamaglia, M.; Mustonen, K.; Tripathi, M.; Mittelberger, A.; Al-Hada, M.; Amati, M.; Sezen, H.; Zeller, P.; Larsen, A. H.; Mangler, C.; Meyer, J. C.; Gregoratti, L.; Bittencourt, C.; Kotakoski, J. Intrinsic core level photoemission of suspended monolayer graphene. *Phys. Rev. Materials* **2018**, *2*, 074005.
 - (11) Bagus, P. S. Self-Consistent-Field Wave Functions for Hole States of Some Ne-Like and Ar-Like Ions. *Phys. Rev.* **1965**, *139*, A619–A634.
 - (12) Pueyo Bellafont, N.; Álvarez Saiz, G.; Viñes, F.; Illas, F. Performance of Minnesota functionals on predicting core-level binding energies of molecules containing main-group elements. *Theor. Chem. Acc.* **2016**, *135*, 35.
 - (13) Susi, T.; Mowbray, D. J.; Ljungberg, M. P.; Ayala, P. Calculation of the graphene C 1s core level binding energy. *Phys. Rev. B* **2015**, *91*, 081401.
 - (14) Pueyo Bellafont, N.; Bagus, P. S.; Illas, F. Prediction of core level binding energies in density functional theory: Rigorous definition of initial and final state contributions and implications on the physical meaning of Kohn-Sham energies. *J. Chem. Phys.* **2015**, *142*, 214102.
 - (15) Pueyo Bellafont, N.; Viñes, F.; Illas, F. Performance of the TPSS Functional on Predicting Core Level Binding Energies of Main Group Elements Containing Molecules: A Good Choice for Molecules Adsorbed on Metal Surfaces. *J. Chem. Theory Comput.* **2016**, *12*, 324–331.
 - (16) Kahk, J. M.; Lischner, J. Accurate absolute core-electron binding energies of molecules, solids, and surfaces from first-principles calculations. *Phys. Rev. Materials* **2019**, *3*, 100801.
 - (17) Golze, D.; Wilhelm, J.; van Setten, M. J.; Rinke, P. Core-Level Binding Energies from GW: An Efficient Full-Frequency Approach within a Localized Basis. *J. Chem. Theory Comput.* **2018**, *14*, 4856–4869.
 - (18) Michelitsch, G. S.; Reuter, K. Efficient simulation of near-edge x-ray absorption fine structure (NEXAFS) in density-functional theory: Comparison of core-level constraining approaches. *J. Chem. Phys.* **2019**, *150*, 074104.
 - (19) Ozaki, T.; Lee, C.-C. Absolute Binding Energies of Core Levels in Solids from First Principles. *Phys. Rev. Lett.* **2017**, *118*, 026401.
 - (20) Kahk, J. M.; Lischner, J. Core electron binding energies of adsorbates on Cu(111) from first-principles calculations. *Phys. Chem. Chem. Phys.* **2018**, *20*, 30403–30411.
 - (21) Pueyo Bellafont, N.; Viñes, F.; Hieringer, W.; Illas, F. Predicting core level binding energies shifts: Suitability of the projector augmented wave approach as implemented in VASP. *J. Comput. Chem.* **2017**, *38*, 518–522.
 - (22) Pehlke, E.; Scheffler, M. Evidence for site-sensitive screening of core holes at the Si and Ge (001) surface. *Phys. Rev. Lett.* **1993**, *71*, 2338–2341.
 - (23) Köhler, L.; Kresse, G. Density functional study of CO on Rh(111). *Phys. Rev. B* **2004**, *70*, 165405.
 - (24) Olovsson, W.; Göransson, C.; Pourovskii, L. V.; Johansson, B.; Abrikosov, I. A. Core-level shifts in fcc random alloys: A first-principles approach. *Phys. Rev. B* **2005**, *72*, 064203.
 - (25) Bagus, P. S.; Nelin, C. J.; Zhao, X.; Levchenko, S. V.; Davis, E.; Weng, X.; Späth, F.; Papp, C.; Kuhlenbeck, H.; Freund, H.-J. Revisiting surface core-level

- shifts for ionic compounds. *Phys. Rev. B* **2019**, *100*, 115419.
- (26) Zheng, X.; Cheng, L. Performance of Delta-Coupled-Cluster Methods for Calculations of Core-Ionization Energies of First-Row Elements. *J. Chem. Theory Comput.* **2019**, *15*, 4945–4955.
- (27) Holme, A.; Børve, K. J.; Sæthre, L. J.; Thomas, T. D. Accuracy of Calculated Chemical Shifts in Carbon 1s Ionization Energies from Single-Reference ab Initio Methods and Density Functional Theory. *J. Chem. Theory Comput.* **2011**, *7*, 4104–4114.
- (28) Sen, S.; Shee, A.; Mukherjee, D. Inclusion of orbital relaxation and correlation through the unitary group adapted open shell coupled cluster theory using non-relativistic and scalar relativistic Hamiltonians to study the core ionization potential of molecules containing light to medium-heavy elements. *J. Chem. Phys.* **2018**, *148*, 054107.
- (29) Liu, J.; Matthews, D.; Coriani, S.; Cheng, L. Benchmark Calculations of K-Edge Ionization Energies for First-Row Elements Using Scalar-Relativistic Core-Valence-Separated Equation-of-Motion Coupled-Cluster Methods. *J. Chem. Theory Comput.* **2019**, *15*, 1642–1651.
- (30) Voora, V. K.; Galhenage, R.; Hemminger, J. C.; Furche, F. Effective one-particle energies from generalized Kohn-Sham random phase approximation: A direct approach for computing and analyzing core ionization energies. *J. Chem. Phys.* **2019**, *151*, 134106.
- (31) Hedin, L. New Method for Calculating the One-Particle Green's Function with Application to the Electron-Gas Problem. *Phys. Rev.* **1965**, *139*, A796–A823.
- (32) Golze, D.; Dvorak, M.; Rinke, P. The GW compendium: A practical guide to theoretical photoemission spectroscopy. *Front. Chem.* **2019**, *7*, 377.
- (33) Govoni, M.; Galli, G. Large Scale GW Calculations. *J. Chem. Theory Comput.* **2015**, *11*, 2680–2696.
- (34) Wilhelm, J.; Del Ben, M.; Hutter, J. GW in the Gaussian and Plane Waves Scheme with Application to Linear Acenes. *J. Chem. Theory Comput.* **2016**, *12*, 3623–3635.
- (35) Wilhelm, J.; Hutter, J. Periodic GW calculations in the Gaussian and plane-waves scheme. *Phys. Rev. B* **2017**, *95*, 235123.
- (36) Wilhelm, J.; Golze, D.; Talirz, L.; Hutter, J.; Pignedoli, C. A. Toward GW Calculations on Thousands of Atoms. *J. Phys. Chem. Lett.* **2018**, *9*, 306–312.
- (37) Ben, M. D.; da Jornada, F. H.; Canning, A.; Wichmann, N.; Raman, K.; Sasanka, R.; Yang, C.; Louie, S. G.; Deslippe, J. Large-scale GW calculations on pre-exascale HPC systems. *Comput. Phys. Commun.* **2019**, *235*, 187–195.
- (38) Zhou, J. S.; Kas, J. J.; Sponza, L.; Reshetnyak, I.; Guzzo, M.; Giorgetti, C.; Gatti, M.; Sottile, F.; Rehr, J. J.; Reining, L. Dynamical effects in electron spectroscopy. *J. Chem. Phys.* **2015**, *143*, 184109.
- (39) Aoki, T.; Ohno, K. Accurate quasiparticle calculation of x-ray photoelectron spectra of solids. *J. Phys.: Condens. Matter* **2018**, *30*, 21LT01.
- (40) van Setten, M. J.; Costa, R.; Viñes, F.; Illas, F. Assessing GW Approaches for Predicting Core Level Binding Energies. *J. Chem. Theory Comput.* **2018**, *14*, 877–883.
- (41) van Setten, M. J.; Caruso, F.; Sharifzadeh, S.; Ren, X.; Scheffler, M.; Liu, F.; Lischner, J.; Lin, L.; Deslippe, J. R.; Louie, S. G.; Yang, C.; Weigend, F.; Neaton, J. B.; Evers, F.; Rinke, P. GW100: Benchmarking G_0W_0 for Molecular Systems. *J. Chem. Theory Comput.* **2015**, *11*, 5665–5687.
- (42) Blum, V.; Gehrke, R.; Hanke, F.; Havu, P.; Havu, V.; Ren, X.; Reuter, K.; Scheffler, M. Ab initio molecular simulations with numeric atom-centered orbitals. *Comput. Phys. Commun.* **2009**, *180*, 2175–2196.
- (43) Perdew, J. P.; Burke, K.; Ernzerhof, M. Generalized Gradient Approximation Made Simple. *Phys. Rev. Lett.* **1996**, *77*, 3865–3868.
- (44) Caruso, F.; Rinke, P.; Ren, X.; Scheffler, M.; Rubio, A. Unified description of ground and excited states of finite systems: The self-consistent GW approach. *Phys. Rev. B* **2012**, *86*, 081102(R).
- (45) Caruso, F.; Rinke, P.; Ren, X.; Rubio, A.; Scheffler, M. Self-consistent GW: All-electron implementation with localized basis functions. *Phys. Rev. B* **2013**, *88*, 075105.
- (46) Sankari, R.; Ehara, M.; Nakatsuji, H.; De Fanis, D. A.; Aksela, H.; Sorensen, S. L.; Piancastelli, M. N.; E., K.; Ueda, K. High resolution O 1s photoelectron shake-up satellite spectrum of H₂O. *Chem. Phys. Lett.* **2006**, *422*, 51–57.
- (47) Schirmer, J.; Angonoa, G.; Svensson, S.; Nordfors, D.; Gelius, U. High-energy photoelectron C 1s and O 1s shake-up spectra of CO. *J. Phys. B: At. Mol. Opt. Phys.* **1987**, *20*, 6031–6040.
- (48) Gatti, M.; Panaccione, G.; Reining, L. Effects of Low-Energy Excitations on Spectral Properties at Higher Binding Energy: The Metal-Insulator Transition of VO₂. *Phys. Rev. Lett.* **2015**, *114*, 116402.
- (49) Byun, Y.-M.; Ögüt, S. Practical GW scheme for electronic structure of 3d-transition-metal monoxide anions: ScO⁻, TiO⁻, CuO⁻, and ZnO⁻. *J. Chem. Phys.* **2019**, *151*, 134305.

- (50) Atalla, V.; Yoon, M.; Caruso, F.; Rinke, P.; Scheffler, M. Hybrid density functional theory meets quasiparticle calculations: A consistent electronic structure approach. *Phys. Rev. B* **2013**, *88*, 165122.
- (51) Adamo, C.; Barone, V. Toward reliable density functional methods without adjustable parameters: The PBE0 model. *J. Chem. Phys.* **1999**, *110*, 6158–6170.
- (52) Ernzerhof, M.; Scuseria, G. E. Assessment of the Perdew-Burke-Ernzerhof exchange-correlation functional. *J. Chem. Phys.* **1999**, *110*, 5029–5036.
- (53) Körzdörfer, T.; Marom, N. Strategy for finding a reliable starting point for G_0W_0 demonstrated for molecules. *Phys. Rev. B* **2012**, *86*, 041110.
- (54) Aoki, T.; Ohno, K. Ab initio simulations of x-ray emission spectroscopy with the GW +Bethe-Salpeter equation method. *Phys. Rev. B* **2019**, *100*, 075149.
- (55) Dunning, T. H. Gaussian basis sets for use in correlated molecular calculations. I. The atoms boron through neon and hydrogen. *J. Chem. Phys.* **1989**, *90*, 1007–1023.
- (56) Wilson, A. K.; van Mourik, T.; Dunning, T. H. Gaussian basis sets for use in correlated molecular calculations. VI. Sextuple zeta correlation consistent basis sets for boron through neon. *J. Mol. Struct. (Theochem)* **1996**, *388*, 339–349.
- (57) Ambrose, M. A.; Jensen, F. Probing Basis Set Requirements for Calculating Core Ionization and Core Excitation Spectroscopy by the Δ Self-Consistent-Field Approach. *J. Chem. Theory Comput.* **2019**, *15*, 325–337.
- (58) van Lenthe, E.; Baerends, E. J.; Snijders, J. G. Relativistic total energy using regular approximations. *J. Chem. Phys.* **1994**, *101*, 9783–9792.
- (59) Salpeter, E. E.; Bethe, H. A. A Relativistic Equation for Bound-State Problems. *Phys. Rev.* **1951**, *84*, 1232–1242.
- (60) Havu, V.; Blum, V.; Havu, P.; Scheffler, M. Efficient $O(N)$ integration for all-electron electronic structure calculation using numeric basis functions. *J. Comput. Phys.* **2009**, *228*, 8367–8379.
- (61) Ren, X.; Rinke, P.; Blum, V.; Wieferink, J.; Tkatchenko, A.; Sanfilippo, A.; Reuter, K.; Scheffler, M. Resolution-of-identity approach to Hartree-Fock, hybrid density functionals, RPA, MP2 and GW with numeric atom-centered orbital basis functions. *New J. Phys.* **2012**, *14*, 053020.
- (62) Tkatchenko, A.; Scheffler, M. Accurate Molecular Van Der Waals Interactions from Ground-State Electron Density and Free-Atom Reference Data. *Phys. Rev. Lett.* **2009**, *102*, 073005.
- (63) Weigend, F.; Ahlrichs, R. Balanced basis sets of split valence, triple zeta valence and quadruple zeta valence quality for H to Rn: Design and assessment of accuracy. *Phys. Chem. Chem. Phys.* **2005**, *7*, 3297–3305.
- (64) Foster, J. M.; Boys, S. F. Canonical Configurational Interaction Procedure. *Rev. Mod. Phys.* **1960**, *32*, 300–302.
- (65) Holzer, C.; Klopper, W. Ionized, electron-attached, and excited states of molecular systems with spin-orbit coupling: Two-component GW and Bethe-Salpeter implementations. *J. Chem. Phys.* **2019**, *150*, 204116.
- (66) Čertík, O.; Pask, J. E.; Vackář, J. dftatom: A robust and general Schrödinger and Dirac solver for atomic structure calculations. *Comput. Phys. Commun.* **2013**, *184*, 1777–1791.